

COMPARISON OF FATIGUE CRACK PROPAGATION MODELS FOR SAC 50 STRUCTURAL STEEL WELDED JOINTS

Geraldo de Paula Martins, gpm@cdtn.br

Researcher of Nuclear Technology Development Center/Nuclear Energy national Commission, CDTN/CNEN, Belo Horizonte, Minas Gerais Brazil

Jefferson José Villela, jjv@cdtn.br

Researcher of Nuclear Technology Development Center/Nuclear Energy National Commission, CDTN/CNEN, Belo Horizonte, Minas Gerais Brazil

Emerson Giovanni Rabello, egr@cdtn.br

Researcher of Nuclear Technology Development Center/Nuclear Energy National Commission, CDTN/CNEN, Belo Horizonte, Minas Gerais Brazil

Carlos Alberto Cimini Jr., cimini@ufmg.br

Professor of Mechanical Engineering Department, Federal University of Minas Gerais, Belo Horizonte, Minas Gerais, Brazil

Leonardo Barbosa Godefroid, leonardo@demet.em.ufop.br

Professor of Metallurgical Engineering, Federal University of Ouro Preto, Ouro Preto, Minas Gerais, Brazil

Abstract. In this work fatigue crack propagation resistance was studied by using compact tension specimens of SAC 50 structural steel welded joints with 12 mm in thickness. Hardness measurements at superficial and transversal through thickness on the Base Metal (BM), Heat Affected Zone (HAZ) and Melted Zone (MZ) were made and the results were compared with the yield stress in each one of the three regions. From this, a relationship between hardness and yield stress was obtained. Fatigue crack propagation tests were accomplished using specimens with notch located at the BM, HAZ and MZ. At the HAZ, it was observed a high dispersion. This is due to the several regions that are obtained at the HAZ. Some specimens were submitted to stress relief heat treatment (SRHT) before fatigue crack propagation tests. It was observed a compression residual stress relieve at HAZ. Some propagation crack models were compared, for the BM, HAZ and MZ. It was concluded that the models, which reach all the three regions of crack growth rate fit well to data.

Keywords: fatigue, welded joints, crack propagation fracture

1. INTRODUCTION

Due to the Brazilian technological developing, the manufactures of metallic structures have been claimed for high mechanical strength and atmospheric corrosion steels, needing also to present good weldability. The SAC 50 steels verify these requirements. Such steels have the property of to develop on his surface an oxide layers, that is adherent to the metallic substrate, when exposed to the industrial atmospheric mean.

The higher resistance of these steels enables reduction in weigh, economy of welds transports, and others advantages. The elevated resistance to atmospheric corrosion results in a major durability.

In this work the behavior of welded structures of SAC 50 steel relative to crack propagation is studied. With the obtained results, mathematical models relating crack propagation rate with the fracture toughness are compared. The Paris laws coefficients and exponents are obtained from the crack propagation tests for the three regions (BM, HAZ and MZ) with 95% confidence, using regression analyses.

1.1. Fatigue Crack Propagation

Fatigue crack propagation make uses of fracture mechanics concepts, in general, the stress intensity factor range defined as (Anderson, 2005):

$$\Delta K = K_{\max} - K_{\min} = \Delta \sigma \sqrt{\pi a} f\left(\frac{a}{W}\right) \quad (1)$$

The fatigue crack propagation rate is defined as the crack extension ratio Δa , by the cycle number, ΔN , that is, $\Delta a/\Delta N$. At the limit,

$$\lim_{\Delta N \rightarrow 0} \frac{\Delta a}{\Delta N} = \frac{da}{dN} \quad (2)$$

When the ratio $R = \sigma_{\min}/\sigma_{\max}$ is the same, ΔK correlates crack propagation rates in specimens with different stress ranges and crack length, and also specimens of different geometry, that is,

$$\frac{da}{dN} = f(\Delta K, R) \quad (3)$$

Figure 1 is a schematic log-log plot of $da/dN \times \Delta K$, which illustrates typical fatigue crack propagation behavior in metals. The curve has a sigmoidal appearance and contains three distinct regions. At intermediate ΔK values, the curve is linear (region II), but the crack propagation rate deviates from the linear trend at high and low ΔK levels. At low end, da/dN approaches zero at a value of ΔK , known as ΔK_{th} , the value below which the crack will not propagate.

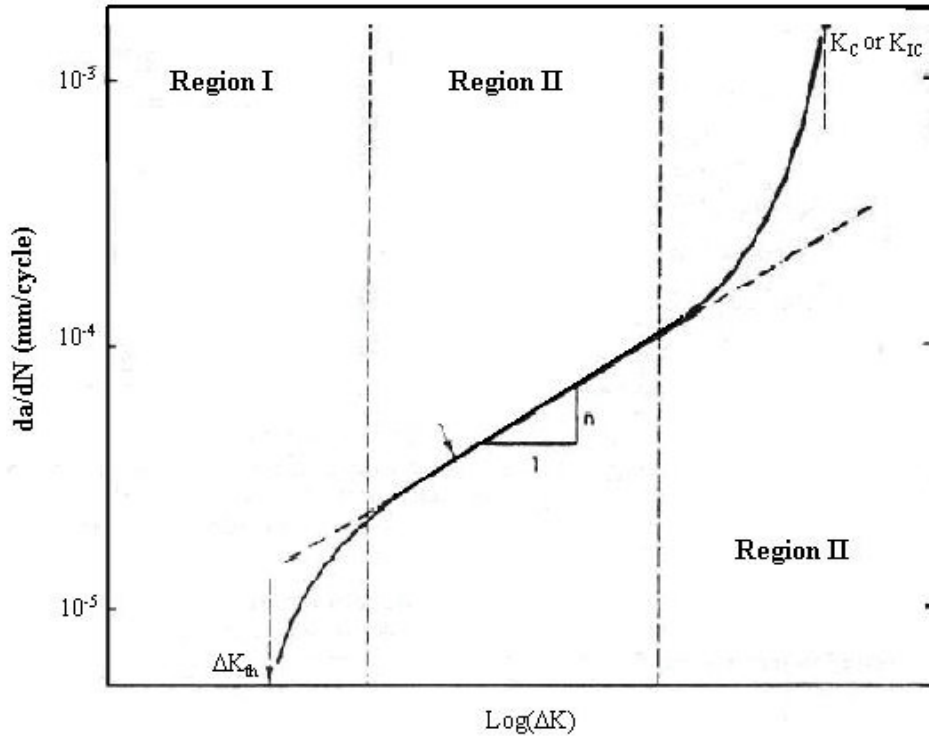


Figure 1: Typical fatigue crack propagation behavior in metals (Adapted from Anderson, 2005)

Several equations describing the behavior of crack propagation involving constants of the material, loading rate and actuating level stress were proposed (Godefroid, Cândido and Moraes, 2004). The models presented in this work are:

Paris model: Paris (1961) and Paris and Erdogan (1960) were the firsts to find a relationship type power laws to describe the fatigue crack growth at the region II. They proposed a empirical relationship presented bellow (Eq. 4), where C and n are constants of the material, experimentally determined:

$$\frac{da}{dN} = C(\Delta K)^n \quad (4)$$

Priddle model: Priddle (1976) had developed a valid relationship for regions I, II and III, where the threshold value of ΔK is not a constant, but depends on the rate R . Such relationship consider the power laws behavior at high and low values of ΔK ; C and n are constants of the material.

$$\frac{da}{dN} = C \left(\frac{\Delta K - \Delta K_{th}}{K_C - K_{max}} \right)^n \quad (5)$$

Colliepriest model: relationship developed by Colliepriest (Barroso, 2004) valid for the three regions I, II e III:

$$\text{Log} \left(\frac{da}{dN} \right) = C_1 + C_2 \tan^{-1} h \left[\frac{\text{Log} \left(\frac{\Delta K^2}{K_{th} K_C (1-R)^2} \right)}{\text{Log} \left(\frac{K_C}{K_{th}} \right)} \right] \quad (6)$$

C_1 and C_2 are parameters to be determined for each material; K_C is the critical value of K and K_{th} is the value below which the crack will not propagate.

2. METHODOLOGY

The material used in this work was the SAC 50 structural steel, employed on building, bridges and other applications, 12mm in thickness.

On the Tab. 1 is presented the chemical compositions supplied by the manufacturer.

Table 1: Chemical composition of SAC 50 steel, 12mm in thickness

Elements (% in weight)										
C	Mn	Si	P	S	Al	Cu	Nb	Ti	Cr	Ni
0.12	1.13	0.34	0.024	0.013	0.037	0.26	0.022	0.009	0.44	0.20

The welding process used was the shielded metal arc welding, according AWS. Some joints were prepared with V bevel for fatigue crack propagation specimens with notch localized at the MZ and other joints were prepared with 1/2V bevel for fatigue crack propagation specimens with notch localized on the HAZ.

On Fig 2 is presented the scheme for removal of fatigue crack propagation tests specimens.

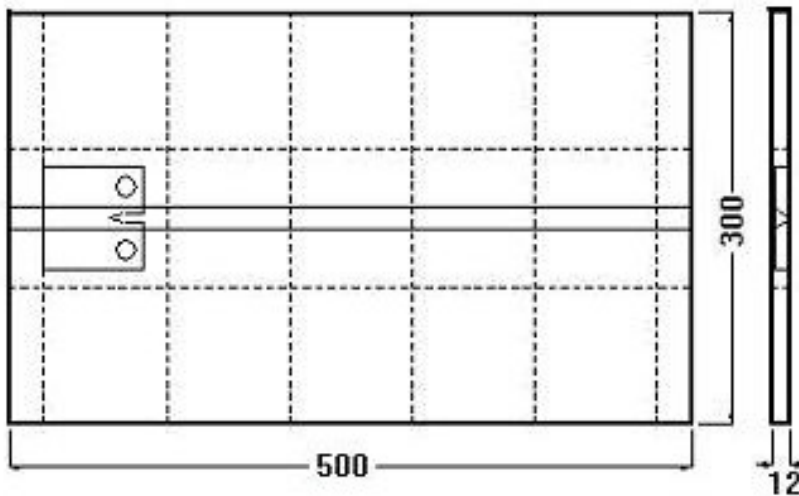


Figure 2: Scheme for removal of fatigue crack propagation tests specimens

Some specimens were submitted to stress relief heat treatment, and submitted to Vickers hardness measurements before and after SRHT. The purpose of this is to observe the influence of the SRHT on the fatigue crack propagation.

The purpose of Vickers hardness measurements is to compare the results with the yield stress in each region (BM, HAZ and MZ).

The specimens for fatigue crack propagation tests were prepared according ASTM E 647 (2000) and are presented in Fig 3.

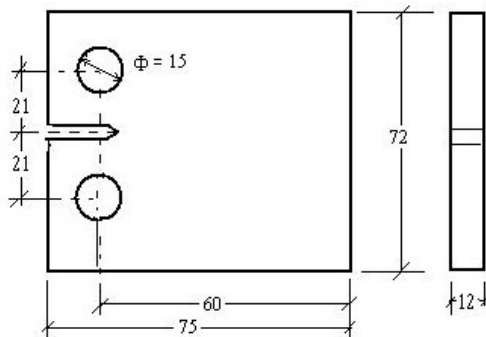


Figure 3: Specimen for fatigue crack propagation; dimensions in mm

3. RESULTS AND DISCUSS

The mechanical properties (yield stress and ultimate stress) were determined in another work by Martins, Cimini and Godefroid (2001) and are presented on Tab 2.

Table 2: Mean values of yield stress and ultimate stress (longitudinal and transverse values) for welded joints

Orientation	0.2% Yield stress (MPa)	Ultimate stress (MPa)
Longitudinal	537.33 ± 14.34	681.33 ± 8.25
Transverse	480.00 ± 8.16	597.67 ± 8.16

3.1. Vickers Hardness Measurement Results

On Fig. 4 are presented the positions of the Vickers hardness (HV) measurements results realized on the welded joints. On the Tab. 3 are presented the mean and standard deviation for each region.

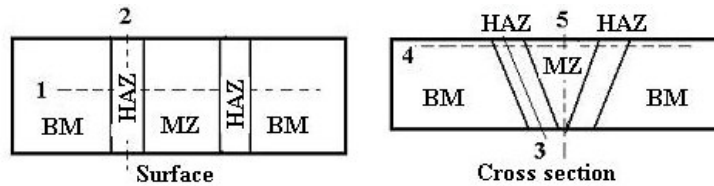


Figure 4: Positions of Vickers hardness measurements

Table 3: Means of Vickers hardness measurements

Region	Mean ± standard deviation
BM	177.31±5.38
HAZ	203.13±13.98
MZ	213.87±6.50

As can be observed, the hardness on the HAZ presented a higher dispersion, and in the BM, the values are smaller than the values obtained in the HAZ and MZ.

On Fig. 5 is presented a scheme of Vickers microhardness measurements using loads of 0.98N in specimens from weld bead. The mean values and standard deviation are presented on Tab.4

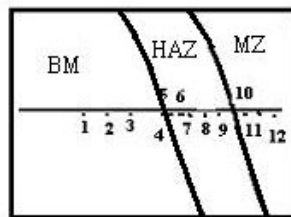


Figure 5: Positions of Vickers microhardness measurements

Table 4: Means and standard deviation of Vickers microhardness from weld bead

Region	Mean ± standard deviation
BM	221.33 ± 9.74
HAZ	237.00 ± 22.41
MZ	254.00 ± 17.85

The values of microhardness were higher than the values obtained for Vickers hardness on the BM and on the MZ, probably, due to the small dimensions of the indenter in comparison with the indenter for hardness measurements, associated to the smaller hard compound of carbides.

Other hardness measurements were made beside the crack trajectory, transverse to crack propagation direction in specimens AW, and in specimens that were submitted to SRHT. The means and standard deviation results are presented on Tab. 5.

Table 5: Mean values of hardness, obtained at several regions AW and with SRHT

Localization		BM	HAZ	MZ
Condition	AW	212.0±9.1	252.0±18.3	298.9±32.7
	SRHT		230.0±25.9	239.7±16.2

As can be observed, after SRHT, there was a decreasing on the hardness values. The several values of Vickers hardness measurements and the yield stresses values for BM, HAZ and MZ, can be related. The yield stress values are: BM: $\sigma_e=442.9\pm 7.8$ MPa (Alcântara, 2003); HAZ: 480.0 ± 8.2 ; MZ: $597,7 \pm 8.2$ (Martins, Cimini and Godefroid, 2001); From linear regression analysis, the relationship between Vickers hardness and yield stress were obtained (Eq. 8):

$$\sigma_y = 2.25HV \tag{7}$$

The maximum variation observed in this relationship were 20% that can be considered good for empirical correlation

3.2. Crack Propagation Tests Results

On Fig. 6 is presented the fatigue propagation curves $da/dN \times \Delta K_{eff}$ for BM (Fig. 6a), HAZ (Fig. 6b) and MZ (Fig 6c), according ASTM E 647 (2000). The K_{eff} values were obtained from the relation proposed by Kumar and Singh (1985) for ferritic steels, that is $\Delta K_{eff} = (0.75+0.25R)\Delta K$.

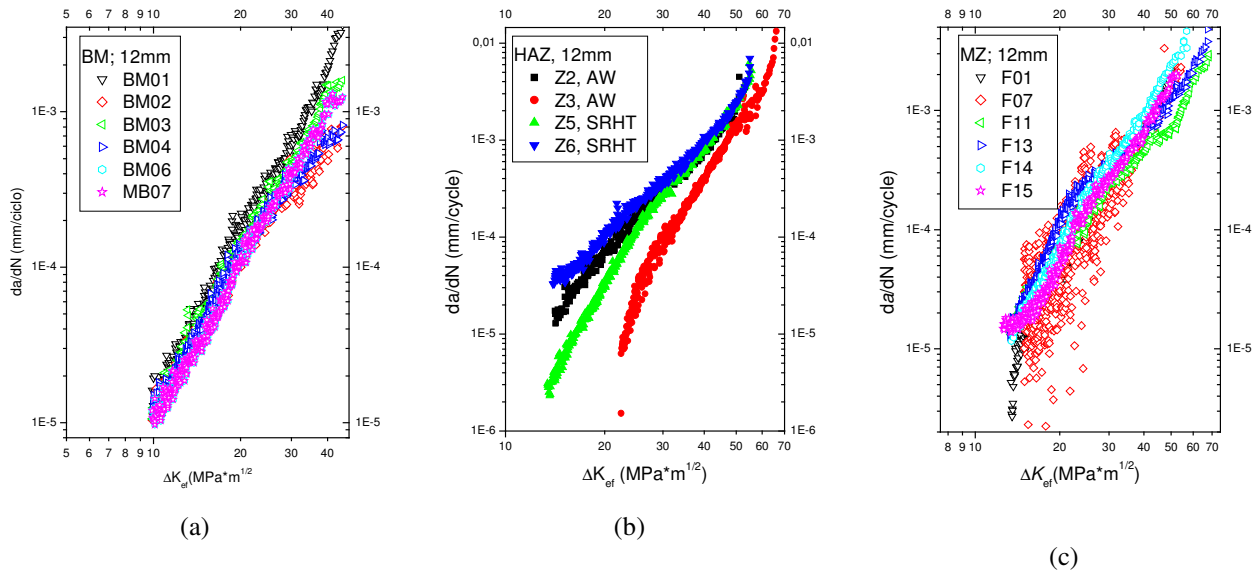


Figure 6: Graphic of $da/dN \times \Delta K_{eff}$; (a): BM, stress ratio, $R=0.1$; amplitude: 3.6kN; (b): HAZ stress ratio = 0.1, amplitude = 4.6kN; (c): MZ; stress ratio = 0.1, amplitude = 4.6

As can be observed, the specimens BM02 and BM04, present a small retardation on the crack propagation, at values of ΔK_{ef} between 30 and 40 $MPa\sqrt{m}$. According Lal (1996), probably, this is due, to the microstructure variations at the rolling transverse orientation evolving combined effects of Young modulus and ratio stress. The specimens Z5, Z6 (Fig 6b), F13, F14 and F15 (Fig. 6c), that were submitted to SRHT presented a smaller crack propagation rate. Probably, the stresses due to welding were tension stresses and after SRHT these tension were relieved.

3.3. Determination of the Coefficients and Exponents from Regression Analysis

The obtainment of the coefficients (C) and exponents (n) of Paris-Erdogan Eq., from regression analysis were realized from the tests data with 95% confidence. From the Eq. 8:

$$\frac{da}{dN} = C(\Delta K_{eff})^n \tag{8}$$

$$\text{Log}\left(\frac{da}{dN}\right) = \text{Log}(C) + n\text{Log}(\Delta K_{eff}) \tag{9}$$

Eq. type:

$$Y = A + nX \tag{10}$$

On the Tab. 6 are presented the values of C and n for the several groups MB, Z (AW), Z (SRHT), ZF (AW) and ZF (SRHT)

Table 6: Coefficients (C) and exponents (n) values of Paris Eq. with 95% confidence

Groups	Coefficients C values			Exponents n values		
	Mean	95% Inferior	95% Superior			
MB	4.487×10^{-9}	4.235×10^{-9}	4.753×10^{-9}	3.430	3.411	3.450
Z(AW)	1.120×10^{-9}	6.856×10^{-10}	1.903×10^{-9}	3.486	3.330	3.642
Z(SRHT)	8.963×10^{-10}	6.121×10^{-10}	1.313×10^{-10}	3.742	3.624	3.859
ZF(AW)	4.999×10^{-9}	4.093×10^{-9}	6.105×10^{-9}	3.164	3.102	3.226
ZF(SRHT)	1.595×10^{-9}	1.395×10^{-9}	1.823×10^{-9}	3.559	3.518	3.601

As can be observed, the coefficient values for the groups AW and SRHT, indicate that the specimens AW, presents propagation rates smaller than the specimens that were submitted to SRHT. This is, probably, due to the effect of the SRHT had compressed residual stresses relieved, favoring the crack propagation at that region.

According Barson and Rolfe (1999), typical values of the Paris law coefficients C and exponents n, for ferritic steels are respectively 3.6×10^{-10} and 3. In this work, the values are in accordance with the values proposed by Barson and Rolfe.

3.4. Comparison of Crack Propagation Models

The Paris-Erdogan model is applicable only for the region II of the $da/dN \times \Delta K_{eff}$ curve. As presented in this work, other models are applicable to the two or to the three regions, but it is necessary to know the K_C or K_{th} values for each case. On Fig. 7 are presented the curves for the specimens BM01, Z5 and MZ01, obtained from tests and the curves adjusted for each one of the three models: Paris-Erdogan, Priddle and Colliepriest and on Tab. 7 is presented the corresponding equations for Paris-Erdogan model for region II and Priddle and Colliepriest models for the three regions

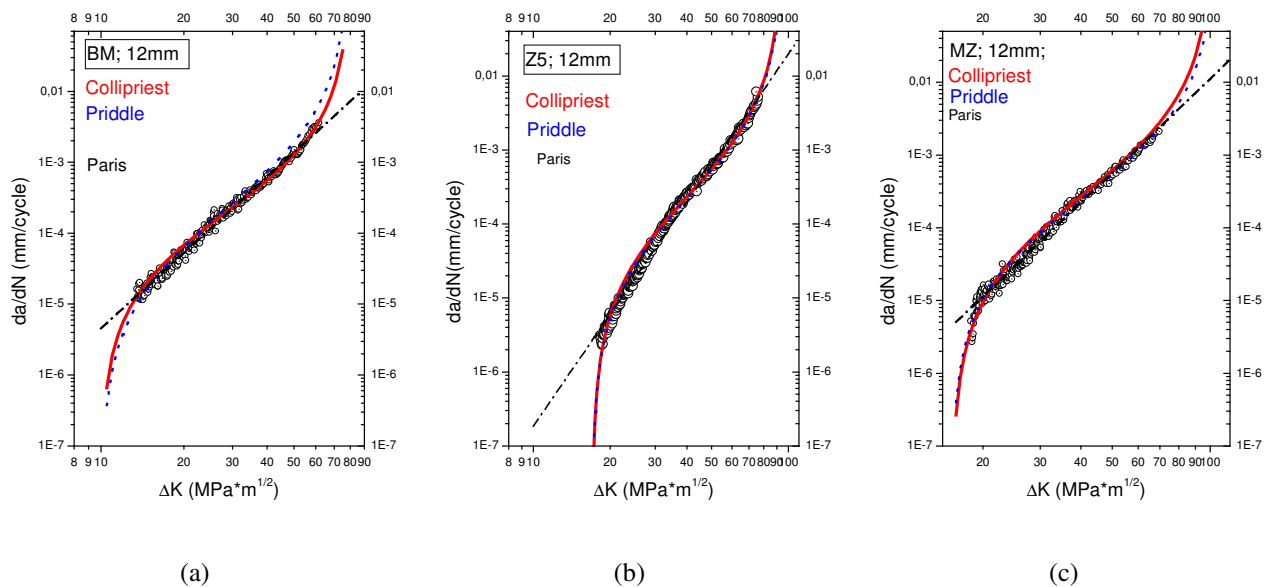


Figure 7: Fatigue crack propagation models: (a) BM; (b) HAZ; (c) MZ

Table 7: Equations for fatigue crack propagation models for the specimens BM01, Z5 and F01

Model	Region		
	BM	HAZ	MZ
Paris	$\frac{da}{dN} = 3.94 \times 10^{-9} (\Delta K_{eff})^{3.54}$	$\frac{da}{dN} = 5.5 \times 10^{-9} (\Delta K)^{3.82}$	$\frac{da}{dN} = 1.17 \times 10^{-10} (\Delta K)^{4.28}$
Priddle	$\frac{da}{dN} = 1.41 \times 10^{-3} \left(\frac{\Delta K - 8}{88 - k_{max}} \right)^{1.64}$	$\frac{da}{dN} = 1.08 \times 10^{-3} \left(\frac{\Delta K - 17}{106 - K_{max}} \right)^{1.59}$	$\frac{da}{dN} = 1.28 \times 10^{-3} \left(\frac{\Delta K - 16}{114 - K_{max}} \right)^{1.54}$
Colliepriest	$\text{Log} \left(\frac{da}{dN} \right) = -3.71 + 1.33 \tan^{-1} h \left[\frac{\text{Log} \left(\frac{\Delta K^2}{800} \right)}{\text{Log}(8.0)} \right]$	$\text{Log} \left(\frac{da}{dN} \right) = -3.62 + 1.43 \tan^{-1} h \left[\frac{\text{Log} \left(\frac{\Delta K^2}{1621} \right)}{\text{Log}85.6} \right]$	$\text{Log} \left(\frac{da}{dN} \right) = -3.55 + 1.48 \tan^{-1} h \left[\frac{\text{Log} \left(\frac{\Delta K^2}{1642} \right)}{\text{Log}(6.4)} \right]$

Calculations using numerical integration for each one of the three models of the Tab. 7 were made and compared with the real data obtained from the tests. The Colliepriest and Priddle models presented results near the data of the tests for the three specimens and the results are presented on Tab. 8.

Table 8: Number of cycles obtained from the tests and from Paris, Priddle and Colliepriest models

Specimen	Tests	Models		
		Paris-Erdogan	Priddle	Colliepriest
BM01	528000	201992	532193	528051
Z5	827000	184036	804412	827612
F01	1410000	232973	1429033	1415472

As can be observed, the Priddle and Colliepriest models supplied results near the real data and the Paris-Erdogan model is very conservative, because on the region I, the crack propagation rate is very slow, and the behavior is not linear as furnished by Paris-Erdogan model.

4. CONCLUSIONS

The hardness results measurements obtained in the specimens with the notch localized on the HAZ and MZ were higher than the results obtained on the specimens with notch localized on the BM;

Comparison of mean hardness measured with the yield stresses for the three regions allow to stablish a correlation between hardness and yield stress, and the relationship obtained were $\sigma_y = 2.25\text{HV}$ with 20% maximum of variation;

The SRHT realized in specimens with notch localized on the HAZ and on the MZ relieved compression stresses and the crack propagation rate were higher than the obtained on specimens AW.

The comparison of fatigue crack propagation models with the real data, the Priddle and Colliepriest models adjusted well with the data, and the application of the Paris-Erdogan model showed to be very conservative for specimens with crack that presents a curve with region I. The Paris-Erdogan model must be employed when the crack size is not small, when the behavior presents a $da/dN \times \Delta K$ curve only with the region II (region I suppressed).

5. REFERENCES

- Alcântara, F. L., 2003, "Comportamento do Crescimento de Trinca por Fadiga de um Aço do Tipo USI-SAC-50 Laminado a Quente em Diferentes Espessuras" Dissertação de Mestrado, Pontificia Universidade Católica de Minas Gerais, Belo Horizonte, MG,
- Anderson, T. L., 2005, "Fracture Mechanics Fundamentals and Applications", CRC Taylor & Francis Group, third Ed. New York, USA, 621p.
- ASTM 647, 2000, "Standard Method for Measurement of Fatigue Crack Growth Rates", Philadelphia, USA
- Barroso, E. K. L., 2004, "Efeito da Pré-Deformação e Shot Peening na Tenacidade à Fratura e Propagação de Trinca por Fadiga da Liga de Alumínio 7475-T7351, da Aplicação Aeronáutica", Dissertação de Mestrado, Universidade Federal de Ouro Preto, Programa de Pós Graduação em Engenharia de Materiais, Ouro Preto, MG, Brasil.
- Godefroid, L. B., Cândido, L. C., e Moraes, W. W.; 2004, "Análise de Falhas", Curso da ABM, 30 de agosto a 03 de setembro de 2004, Belo Horizonte, MG.
- Kumar, R., and Singh, K., 1995, "Influence of Stress Ratio on Fatigue Crack Growth in Mild Steel, Engineering Fracture Mechanics, vol.50, nº 3, pp. 377-384

- Lal, D. N., "A New Mechanistic Approach to Analyzing LEFM Fatigue Crack Growth Behavior of Metals and Alloys", Engineering Fracture Mechanics, vol. 47, n° 3, pp. 379-401.
- Martins, G. P., Cimini Jr., C. A., and Godefroid, L. B., 2001, "Influence of Welding Planar Defects in the Fracture Toughness of Structural Steel. Preliminary Testing, 16th International Conference on Structural Mechanics in Reactor Technology, Washington, USA.
- Paris, P. C., Paris, P. C., Gomes, M. P., and Anderson, W. P., 1961 "A Rational Analytic Theory of Fatigue". The Trend in Engineering, Vol. 13, pp. 9-14.
- Paris, P. C. and Erdogan, F., 1960, "A Critical Analysis of Crack Propagation Laws." Journal of Basic Engineering, Vol. 85, pp. 528-534
- Priddle, E. K., 1976. "High Cycle Fatigue Crack Propagation Under Random and Constant Amplitude Loadings." International Journal of Pressure Vessels and Piping, 4, pp. 89-117.
- Barson, J. M. and Rolfe, S. T., 1999, Fracture and Fatigue Control in Structures. Applications of Fracture mechanics, 3^a ed., Prentice Hall, Inc., Englewood Cliffs, New Jersey, USA.

6. RESPONSIBILITY NOTICE

The authors are the only responsible for the printed included in this paper.